

Three-dimensional behavior of apodized nontelecentric focusing systems

Manuel Martínez-Corral, Laura Muñoz-Escrivá, and Amparo Pons

The scalar field in the focal volume of nontelecentric apodized focusing systems cannot be accurately described by the Debye integral representation. By use of the Fresnel–Kirchhoff diffraction formula it is found that, if the aperture stop is axially displaced, the focal-volume structure is tuned. We analyze the influence of the apodizing function and find that, whereas axially superresolving pupil filters are highly sensitive to the focal-volume reshaping effect, axially apodizing filters are more inclined to the focal-shift effect. © 2001 Optical Society of America

OCIS codes: 050.1940, 220.1230, 050.1220.

1. Introduction

In the past few years many researchers have studied the distribution of light near the focus of an apertured monochromatic converging spherical beam.^{1–12} The paper by Li and Wolf¹³ is particularly notable in this regard. In this paper the authors analyze the three-dimensional (3D) irradiance distribution near the focus when a spherical wave is diffracted by a circular aperture (see Fig. 1), and they obtain

$$I(P) = I_0 \left(1 - \frac{u}{2\pi N_L} \right)^2 \times \left| \int_0^1 \exp\left(-i \frac{1}{2} u \rho^2 \right) J_0(v\rho) \rho d\rho \right|^2, \quad (1)$$

where $N_L = r_{\max}^2/\lambda f$ stands for the so-called Fresnel number of the focusing geometry and I_0 stands for the irradiance at the focal point F . In addition,

$$u = 2\pi N_L \frac{z/f}{1 + z/f}, \quad (2)$$

$$v = 2\pi N_L \frac{r/r_{\max}}{1 + z/f}. \quad (3)$$

From these equations it follows that, when $N_L \rightarrow \infty$, the field is symmetrical around the focal point, as predicted by Lommel's theory.¹ However, for decreasing values of N_L , the point of maximum irradiance moves from its coincidence with the geometrical focus toward the center of the aperture. Moreover, because of the nonlinear relation between the normalized coordinates, u and v , and the actual spatial coordinates, z and r , the symmetry around the focus disappears.

Fewer publications have been devoted to the case of the focal field structure generated by nontelecentric focusing systems, i.e., when a circular aperture, under monochromatic plane-wave illumination, is placed in front of a converging spherical lens. This is a much more interesting and general situation, since in most real focusing setups, such as microscope objectives, the aperture stop does not coincide with the principal plane of the system. This geometry was discussed by Wenzel,¹⁴ who considered only the on-axis irradiance distribution, and also in a paper by Sheppard and Török,¹⁵ where the treatment is generalized to include the irradiance at off-axis points.

In this paper the previously reported results are generalized to the case in which nontelecentric focusing systems are apodized, and we analyze how the apodizing function influences the magnitude of the modifications experienced by the focal volume.

2. Basic Theory

Let us consider a nontelecentric focusing system that is apodized by a radially symmetric, purely absorbing diffracting screen with amplitude transmittance $t(r_0)$ and radial extent r_{\max} , as shown in Fig. 2. An approach to calculate the 3D amplitude distribution in

The authors are with the Departamento de Óptica, Universidad de Valencia, 46100 Burjassot, Spain. M. Martínez-Corral's e-mail address is manuel.martinez@uv.es.

Received 4 August 2000; revised manuscript received 9 March 2001.

0003-6935/01/193164-05\$15.00/0

© 2001 Optical Society of America

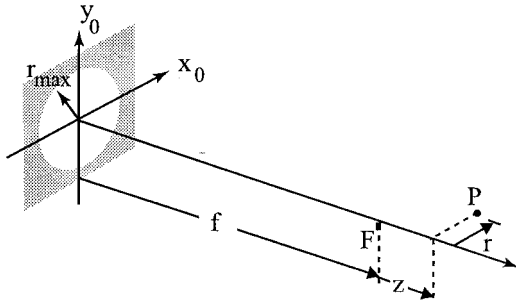


Fig. 1. Schematic representation of the focusing setup. A monochromatic converging spherical wave, with focus at F , illuminates a circular aperture of radius r_{\max} .

the neighborhood of the lens focus is to apply the Fresnel diffraction theory to calculate, first, the amplitude on the lens plane. In a second step this amplitude is used as the input in the Fresnel formula to calculate the amplitude distribution in the focal region. Although this seems to be the natural approach for this calculation,¹⁵ next we consider a more-illustrative procedure. In our approach we first calculate the complex amplitude of the paraxial scalar field at the plane conjugated to the screen plane, which is given by¹⁶

$$U_0(r'_0) = \exp\left(-i \frac{k}{2\zeta'} r_0'^2\right) \frac{1}{|m_0|} t\left(\frac{r'_0}{|m_0|}\right), \quad (4)$$

where m_0 stands for the transverse magnification of the lens.

Note that this amplitude distribution is quite similar to the one that appears when the focal volume generated by a diffracting screen under spherical illumination is studied,¹³ as described in Section 1. Therefore we hypothesize that similar results can be obtained in both situations.

Then, when we proceed as in Ref. 13, i.e., when we use the amplitude $U_0(r'_0)$ as the input in the Fresnel propagation formula, it is straightforward to obtain

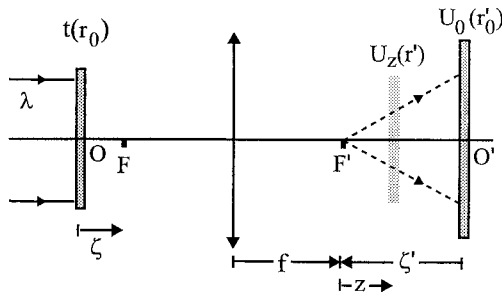


Fig. 2. Schematic layout of a nontelecentric focusing system. At the image plane, O' , the amplitude distribution is given by the product between the geometrical-optics image of the screen and a quadratic phase factor with focus at F' .

the expression for the amplitude distribution in the neighborhood of the focus, namely,

$$U(u, v) = 2\pi N_L \left(1 + \frac{\zeta_N}{2\pi N_L} u\right) \int_0^1 t(\rho) \times \exp\left(-i \frac{1}{2} u \rho^2\right) J_0(v\rho) \rho d\rho, \quad (5)$$

where the maximum value for the radial coordinate ρ has been normalized to unity and the axial position in the focal region is specified through the nondimensional axial variable

$$u = 2\pi N_L \frac{z_N}{1 - z_N \zeta_N}. \quad (6)$$

In the above equations, $z_N = z/f$ and $\zeta_N = \zeta/f$ (see Fig. 2). Parameter $N_L = r_{\max}^2/\lambda f$ represents the Fresnel number of the lens, as defined by Li and Wolf.¹³

The transverse radial coordinate has been expressed through the nondimensional variable

$$v = 2\pi N_L \frac{r_N}{1 - z_N \zeta_N}, \quad (7)$$

where $r_N = r'/r_{\max}$.

Finally, since our aim is to analyze the structure of the 3D irradiance distribution, we write

$$I(u, v) = I_0 \left(1 + \frac{\zeta_N}{2\pi N_L} u\right)^2 \times \left| \int_0^1 t(\rho) \exp\left(-i \frac{1}{2} u \rho^2\right) J_0(v\rho) \rho d\rho \right|^2, \quad (8)$$

where $I_0 = |U(0, 0)|^2$.

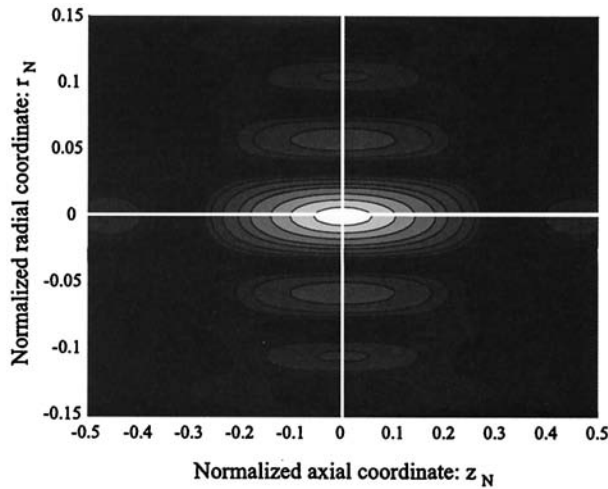
Note that this formula is almost the same as that in Eq. (1). The only difference is that now the irradiance distribution also depends on the parameter ζ_N .

On the basis of Eqs. (6)–(8) the following features about the 3D-field structure can be summarized:

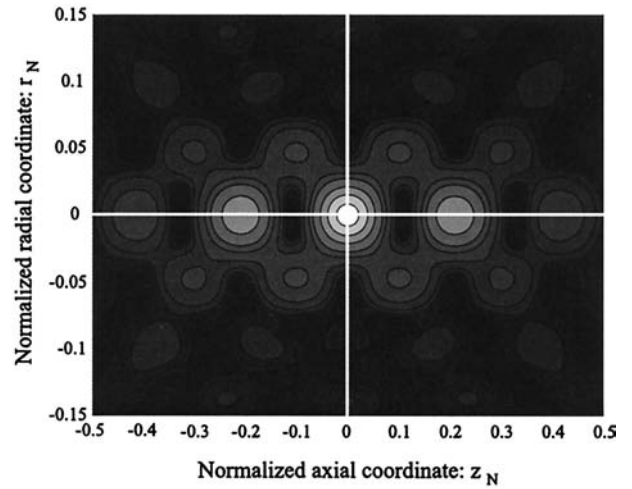
(a) When the focusing system is telecentric ($\zeta_N = 0$), the attenuation factor $(1 + \zeta_N u/2\pi N_L)^2$ reduces to unity, and moreover the variables u and v are proportional to z_N and r_N , respectively. Thus the 3D irradiance distribution is symmetric about the focus. In addition, the scale of the 3D pattern is proportional to $1/N_L$ in both the transverse and the axial directions. Note that this result, which is unobtainable in the focusing geometry of Fig. 1, corresponds to that predicted by the Debye representation of the focal field.¹⁷

(b) When telecentricity is lost ($\zeta_N \neq 0$), the symmetry is broken because the relations between u and v and the actual spatial coordinates are no longer linear. The relations are

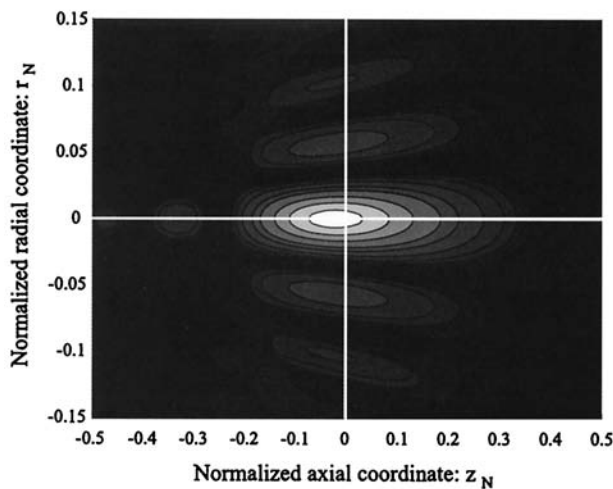
$$z_N = \frac{u}{2\pi N_L + u \zeta_N}, \quad (9)$$



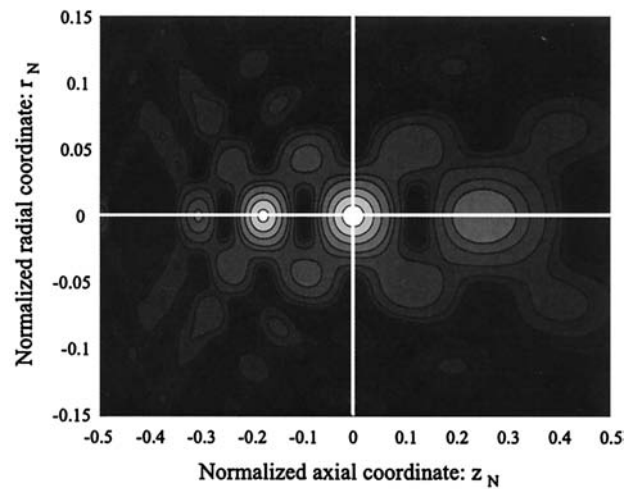
(a)



(a)



(b)



(b)

Fig. 3. Half-toning representation of the numerically evaluated irradiance distribution in the meridian plane corresponding to the axially apodizing filter of Eq. (12): (a) telecentric system and (b) nontelecentric system. The parameters for the calculation were $N_L = 12.25$ and $\zeta_N = 0$ (telecentric) or $\zeta_N = -0.853$ (nontelecentric).

$$r_N = \frac{v}{2\pi N_L + u\zeta_N}. \quad (10)$$

From these nonlinear transformations it is clear that the transverse patterns corresponding to the same modulus of u but different sign will have different scale and that their positions will not be symmetrical about the focus. Specifically, each transverse pattern (defined by the value u) is axially displaced and scaled by a factor

$$M = 1 + \frac{\zeta_N}{2\pi N_L} u. \quad (11)$$

In addition to the break of the symmetry in the diffraction term that is due to the nonlinear coordinate transformations, we should take into account the attenuation factor in Eq. (8). This factor is responsible

Fig. 4. Half-toning representation of the numerically evaluated irradiance distribution in the meridian plane corresponding to the axially superresolving filter of Eq. (13): (a) telecentric system and (b) nontelecentric system. The parameters for the calculation were the same than those of Fig. 3

for the axial displacements of the local maxima and, hence, of the point of maximum irradiance. This is the so-called focal-shift effect.⁵

(c) When we deal with linear and shift-invariant imaging systems, resolution is one of the most important features. It is usual to define resolution in terms of the Rayleigh criterion.¹ According to this criterion the transverse resolution is determined by the width of the central lobe of the transverse irradiance impulse response of the imaging system. The axial resolution is determined by the width of the core of the axial irradiance impulse response. If we consider a nontelecentric imaging system, then its axial and transverse resolutions are determined by the width of the core of $I(z_N, r_N = 0)$ and $I(z_N = 0, r_N)$, respectively. According to the above reasoning it is clear that for any value of ζ_N the transverse resolution is constant and proportional to $1/N_L$ (note that,

for fixed values of r_{\max} and λ , N_L is proportional to the numerical aperture of the system). In contrast, the axial resolution is governed by the value of N_L/ζ_N . Therefore one can conclude that by simple axial displacement of the aperture stop the axial resolution of the system can be tuned while the transverse resolution remains unchanged.

3. Influence of the Pupil Function

In Section 2 we carried out the analysis of the focal structure for nontelecentric focusing systems, but we did not investigate the influence of the pupil function. The analysis revealed in general terms that the farther the pupil filter is from the lens front focal plane (that is, the farther the system is from being telecentric), then the higher the asymmetry induced in the focal volume. Now we address the following question: Is it possible to predict for a given value of N_L when a pupil function is more inclined than other screens to experience reshaping effects? To answer this question, it is necessary to take into account that, when $|\zeta_N|$ increases, a double effect takes place: loss of symmetry and focal shift.

Let us assume that we are dealing with an axially superresolving pupil filter. In this case an axial-irradiance distribution in which the central lobe becomes narrower is produced (compared with that of the circular aperture). This narrowness is accompanied by a severe increase of the strength of the secondary axial sidelobes, which also become narrower. Then this kind of filter produces a focal volume consisting of a set of large out-of-focus lobes. Since these large lobes are centered in points with relatively high value for the axial coordinate, u , they are highly sensitive to the scaling effect. However, if we consider the attenuation term in Eq. (8), we find that this kind of filter is particularly inclined to experience the so-called focal-switch effect,^{18,19} provided that $\zeta_N < 0$, or even an inverse focal-switch effect if $\zeta_N > 0$. Note that the latter effect has never been reported on to our knowledge.

We can conclude that axially superresolving filters, when used as pupil functions in nontelecentric focusing systems, are highly sensitive to the deformation of the diffraction term and are particularly inclined toward the (direct or inverse) focal-switch effect.

Axially apodizing pupil filters produce a widening of the central lobe of the axial-irradiance distribution, which is accompanied by a decreasing strength of the secondary sidelobes. When such filters are used in telecentric focusing systems, a focal volume is obtained in which most of light is concentrated in an ellipsoidal central lobe. Outside this lobe the light density is exceedingly small. Therefore we can state that this kind of filter is not too sensitive to the scaling effect when the system is no longer telecentric. However it is particularly inclined to focal shift, which can be direct or inverse depending on the sign of ζ_N . A paradigmatic example of this statement is a filter with Gaussian transmittance. In such a case, whatever the value of ζ_N , we always obtain a Gaussian beam in the image space. What is governed by

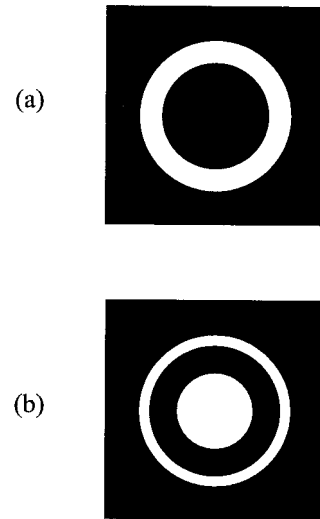


Fig. 5. Actual two-dimensional representation of the binary filters: (a) axially apodizing and (b) axially superresolving.

the value of ζ_N are the waist width and the waist position (i.e., the focal shift).

To illustrate the above reasoning in Figs. 3 and 4, we have represented, in halftone pictures, the irradiance distribution in the meridian plane for two filters and for telecentric and nontelecentric focusing systems.

As an axially apodizing filter we select²⁰

$$t^a(\rho) = \begin{cases} 0 & \text{if } 0 \leq \rho \leq \sqrt{2}/2 \\ 1 & \text{if } \sqrt{2}/2 < \rho \leq 1 \end{cases} \quad (12)$$

The axially superresolving filter is⁸

$$t^s(\rho) = \begin{cases} 1 & \text{if } 0 \leq \rho \leq 1/2 \\ 0 & \text{if } 1/2 < \rho \leq \sqrt{3}/2 \\ 1 & \text{if } \sqrt{3}/2 < \rho \leq 1 \end{cases} \quad (13)$$

In Fig. 5 we have plotted both annular binary filters, which, to allow for a direct comparison of results, have the same light throughput.

Note from Fig. 4 that the large sidelobes produced by the axially superresolving filter are highly sensitive to the reshaping effect. However, the large central lobe produced by the axially apodizing pupil filter (see Fig. 3) is more inclined to the focal-shift effect. It is also remarkable that in this case there is almost no deformation within the central part of the central lobe, and then the focal shift is the only noticeable effect.

4. Conclusions

We have shown that the 3D-irradiance distribution in the focal volume provided by an apodized nontelecentric focusing system is influenced by both the axial position of the apodizer and its amplitude transmittance. Concerning the influence of the apodizing function, we have found that, whereas axially superresolving filters are highly sensitive to the focal-

volume scaling effect and to the focal-switch effect, the axially apodizing filters are more inclined to experience the focal-shift effect.

This research was supported by the Plan Nacional I+D+I (grant DPI2000-0774), Ministerio de Ciencia y Tecnología, Spain.

References

1. M. Born and E. Wolf, *Principles of Optics*, 6th ed. (Pergamon, Oxford, 1987), Chap. 8.
2. J. J. Stammes, *Waves in Focal Regions* (Hilger, Bristol, UK, 1986).
3. M. Gu, *Principles of Three-Dimensional Imaging in Confocal Microscopes* (World Scientific, London, 1996), Chap. 2.
4. P. Jacquino and B. Rozien-Dossier, "Apodisation," in *Progress in Optics*, E. Wolf, ed. (North-Holland, Amsterdam, 1964), Vol. 3.
5. Y. Li and E. Wolf, "Focal shifts in diffracted converging spherical waves," *Opt. Commun.* **39**, 211–215 (1981).
6. S. De Nicola, "On-axis focal shift effects in focused truncated J₀ Bessel beams," *Pure Appl. Opt.* **5**, 827–831 (1996).
7. R. Borghi, M. Santarsiero, and F. Gori, "Axial intensity of apertured Bessel beams," *J. Opt. Soc. Am. A* **14**, 23–26 (1997).
8. M. Martínez-Corral, C. J. Zapata-Rodríguez, P. Andrés, and M. Kowalczyk, "Analytical formula for calculating the focal shift in apodized systems," *J. Mod. Opt.* **45**, 1671–1679 (1998).
9. M. Martínez-Corral, P. Andrés, C. J. Zapata-Rodríguez, and M. Kowalczyk, "Three-dimensional superresolution by annular binary filters," *Opt. Commun.* **165**, 267–278 (1999).
10. E. H. K. Stelzer and S. Grill, "The uncertainty principle applied to estimate focal spot dimensions," *Opt. Commun.* **173**, 51–56 (2000).
11. U. Vokinger, R. Dändliker, P. Blattner, and H. P. Herzig, "Unconventional treatment of focal shift," *Opt. Commun.* **157**, 218–224 (1998).
12. I. G. Palchikova and S. G. Rautian, "The diffractive optical power of a diaphragm," *Opt. Commun.* **174**, 1–5 (2000).
13. Y. Li and E. Wolf, "Three-dimensional intensity distribution near the focus in systems of different Fresnel numbers," *J. Opt. Soc. Am. A* **1**, 801–808 (1984).
14. R. G. Wenzel, "Effect of the aperture-lens separation on the focal shift in large-*F*-number systems," *J. Opt. Soc. Am. A* **4**, 340–345 (1987).
15. C. J. R. Sheppard and P. Török, "Dependence of Fresnel number on aperture stop position," *J. Opt. Soc. Am. A* **15**, 3016–3019 (1998).
16. J. W. Goodman, *Introduction to Fourier Optics*, 2nd ed. (McGraw-Hill, New York, 1996).
17. C. J. Zapata-Rodríguez, P. Andrés, M. Martínez-Corral, and L. Muñoz-Escrivá, "Gaussian imaging transformation for the paraxial Debye formulation of the focal region in a low-Fresnel-number optical system," *J. Opt. Soc. Am. A* **17**, 1185–1191 (2000).
18. M. Martínez-Corral and V. Climent, "Focal switch: a new effect in low Fresnel-number systems," *Appl. Opt.* **35**, 24–26 (1996).
19. Y. Li, "Focal shift and focal switch in dual-focus systems," *J. Opt. Soc. Am. A* **14**, 1297–1304 (1997).
20. W. T. Welford, "Use of annular apertures to increase focal depth," *J. Opt. Soc. Am.* **50**, 749–753 (1960).